arXiv:1704.08064v1 [math.DG] 26 Apr 2017

CARTAN RIBBONIZATION OF SURFACES AND A TOPOLOGICAL INSPECTION

MATTEO RAFFAELLI[1], JAKOB BOHR[2], AND STEEN MARKVORSEN[1]

Abstract. We develop the concept of Cartan ribbons and a method by which they can be used to ribbonize any given surface in space by intrinsically flat ribbons. The geodesic curvature along the center curve on the surface agrees with the geodesic curvature of the corresponding Cartan development curve, and this makes a rolling strategy successful. Essentially, it follows from the orientational alignment of the two co-moving Darboux frames during the rolling. Using closed center curves we obtain closed approximating Cartan ribbons that contribute zero to the total curvature integral of the ribbonization. This paves the way for a particular simple topological inspection – it is reduced to the question of how the ribbons organize their edges relative to each other. The Gauss-Bonnet theorem leads to this topological inspection of the vertices. Finally, we display two examples of ribbonizations of surfaces, namely of a torus using two ribbons, and of an ellipsoid using its closed curvature lines as center curves for the ribbons. The topological inspection of the torus ribbonization is particularly simple as it has no vertex points, giving directly the Euler characteristic 0. The ellipsoid has 4 vertices – corresponding to the 4 umbilical points – each of degree one and each therefore contributing one-half to the Euler characteristic.

1. Introduction

The approximation of surfaces by patch-works of planar parts has a long use in fundamental and applied mathematics. Foremost comes to mind the multifaceted applications of triangulations [1]. In the present work we develop a scheme for approximating a surface by the use of multiple developable surfaces. Some of the beauty of this approach is the relatively few numbers of developable stretches – ribbons – needed to approximate a given surface. Not to mention that the study of shapes and structures of developable surfaces is itself a classical subject that has intrigued mathematicians for centuries and has found numerous artistic applications in architecture and design, see [2] and [3].

In the seventies K. Nomizu pointed out that the concept of (extrinsic) rolling can be understood as a kinematic interpretation of the (intrinsic) Levi-Civita connection and of the Cartan development of curves, see e.g. [4] and [5]. One derives simple expressions for the components of the corresponding relative angular velocity vector of the rolling, i.e. the geodesic torsion, the normal curvature, and the geodesic curvature of the given curve and its development curve, see the works [6, 7, 8, 9]. For example, in conjunction with a plane, the rolling must propagate along a planar curve which has the same geodesic curvature as the given curve, see examples in [10].

In recent years rolling has received a renewed wave of interest – in part because of its importance for robotic manipulation of objects [11]. For example, there has been an interest in understanding rolling from symmetry arguments [12] as well as from purely geometrical considerations [13, 14, 15]. Further, the interesting shapes known as D-forms are examples of surface structures that are formed by assembling several developable surfaces [16, 17, 18].

A topological inspection of ribbonized surfaces with a count of just two terms is developed. Working with closed ribbons makes this inspection especially simple. For example, when building up a ribbonization, the addition of a closed ribbon with no vertex makes zero contribution to the Euler characteristic. Finally, we compare the formula for the Euler characteristic of ribbonizations with the corresponding Morse index formula [19] and the Poincaré-Hopf formula [20].

2. The Initial Setting

We consider two surfaces S and $\tilde{S}$ in $\mathbb{R}^3$. Let γ be a smooth, regular curve on S, $\gamma : J = [0, \alpha] \to S$, such that $\gamma(0) = (0, 0, 0)$. We equip γ with its *Darboux frame field* $\mathcal{F} = \{e, h, N\}$, defined as follows: for each $t \in J$ we let $N(t)$ denote a unit normal vector to S at $\gamma(t)$, we let $e(t) = \gamma'(t)/\|\gamma'(t)\|$ the unit tangent vector of γ and $h(t) = N(t) \times e(t)$. The frame $\mathcal{F}$ then satisfies the following equations – see for example [21, Corollary 17.24]:

$$\begin{bmatrix} e'(t) \\ h'(t) \\ N'(t) \end{bmatrix} = \|\gamma'(t)\| \cdot \begin{bmatrix} 0 & \kappa_g(t) & \kappa_n(t) \\ -\kappa_g(t) & 0 & \tau_g(t) \\ -\kappa_n(t) & -\tau_g(t) & 0 \end{bmatrix} \begin{bmatrix} e(t) \\ h(t) \\ N(t) \end{bmatrix}, \tag{1}$$

where $\tau_g(t)$, $\kappa_n(t)$, and $\kappa_g(t)$ are the geodesic torsion, the normal curvature, and the geodesic curvature, respectively, of γ at $\gamma(t)$. Since we are so far only considering local geometric entities, the surfaces S and $\tilde{S}$ need not be orientable, i.e. the frame $\mathcal{F}$ and its properties – such as the signs appearing in (1) – depend on the local choice of normal vector field N. In the final sections we will note a few consequences concerning the rolling and the corresponding ribbonization of non-orientable surfaces.

3. Moving S on $\tilde{S}$

Given a curve γ on S as above, we now consider smooth and regular curves $\tilde{\gamma}$ on the other surface $\tilde{S}$ such that the following initial compatibility and contact conditions are satisfied:

$$\begin{aligned} \tilde{\gamma}(0) &= \gamma(0) = (0, 0, 0) \\ \tilde{\gamma}'(0) &= \gamma'(0) \\ \|\tilde{\gamma}'\| &= \|\gamma'\| \quad , \end{aligned} \tag{2}$$

so that $\tilde{\gamma}$ has the same initial point and direction as γ and so that $\tilde{\gamma}$ has the same speed as γ for all $t \in J$. A motion of S on $\tilde{S}$ is then defined as follows:

Definition 3.1. Let $E^+(3)$ be the group of direct isometries of $\mathbb{R}^3$. A (1-*parameter*) *motion* f_t *of* S *on* $\tilde{S}$ *along* $\tilde{\gamma}$ is a differentiable map $J \to E^+(3)$ such that f_0 is the identity and such that, for all $t \in J$, the image $f_t(S)$ has the same tangent plane as $\tilde{S}$ at $\tilde{\gamma}(t)$. The point $\tilde{\gamma}(t)$ we call the *contact point* at instant t, and $\tilde{\gamma}(J)$ the *contact curve* of the motion on $\tilde{S}$.

The map f_t is represented by $x \mapsto R_t x + c_t$, where $R_t \in SO(3)$ is a rotation matrix and c_t a vector. The instantaneous motion is then given by the vector field $V_t : x \mapsto \Omega_t(x - c_t) + c_t'$, with $\Omega_t = R_t' R_t^{\mathsf{T}}$, see [4].

We want to find a motion g_t of S on $\tilde{S}$ along $\tilde{\gamma}$ such that $\tilde{\gamma}(t)$ becomes the contact point at instant t. To this end, it suffices to let g_t be the isometry of $\mathbb{R}^3$ taking

$$\begin{aligned} \gamma(t) &\text{ to } \tilde{\gamma}(t), \\ \gamma(t) + e(t) &\text{ to } \tilde{\gamma}(t) + \tilde{e}(t), \\ \gamma(t) + N(t) &\text{ to } \tilde{\gamma}(t) + \tilde{N}(t), \end{aligned} \tag{3}$$

where $\tilde{e}$ and $\tilde{N}$ are two of the members of the Darboux frame $\tilde{\mathcal{F}} = \{\tilde{e}\,,\ \tilde{h} = \tilde{N} \times \tilde{e}\,,\ \tilde{N}\}$ along $\tilde{\gamma}$ on $\tilde{S}$ defined in the same way as the frame $\mathcal{F}$ along γ on S.

Let D_t be the matrix having $e(t)$, $h(t)$ and $N(t)$ as coordinate column vectors (with respect to a fixed coordinate system in $\mathbb{R}^3$) and similarly, let $\tilde{D}_t$ be the matrix having $\tilde{e}(t)$, $\tilde{h}(t)$ and $\tilde{N}(t)$ as coordinate column vectors (with respect to the same fixed coordinate system in $\mathbb{R}^3$). The rotation $\tilde{D}_t D_t^{\mathsf{T}}$ then maps the vector $e(t)$ to $\tilde{e}(t)$, and $N(t)$ to $\tilde{N}(t)$. Using the definition of g_t, one may easily verify that its representation $g_t(x) = R_t x + c_t$ is

$$g_t(x) = \tilde{D}_t D_t^{\mathsf{T}}(x - \gamma(t)) + \tilde{\gamma}(t). \tag{4}$$

4. Rolling S on $\tilde{S}$

A motion g_t of S on $\tilde{S}$ along $\tilde{\gamma}$ is said to be *rotational* if, for all $t \in J$, $V_t(\tilde{\gamma}(t)) = 0$ and Ω_t is different from the zero matrix. At each time instant we can then find a unique vector $\omega_t \neq 0$, the *angular velocity vector*, such that $\omega_t \times x = \Omega_t x$ for all $x \in \mathbb{R}^3$.

Based on the orientation of the angular velocity vector relative to the common tangent space of $g_t(S)$ and $\tilde{S}$, we introduce the following terminology for the instantaneous motion – which extends directly to the entire motion.

Definition 4.1. The instantaneous rotational motion g_t is a *pure spinning* if the angular velocity vector ω_t is orthogonal to the 2D tangent space $T_{\tilde{\gamma}(t)}\tilde{S}$, and a *pure twisting* if ω_t is proportional to the tangent vector $e(t)$. Finally, the motion g_t will be called a *standard rolling* if ω_t does not contain a spinning component and is not a pure twisting, i.e. a standard rolling of S on $\tilde{S}$ is characterized by the condition that there exist smooth functions a and b such that ω_t decomposes as follows for all t:

$$\omega_t = a(t) \cdot \tilde{e}(t) + b(t) \cdot \tilde{h}(t) + 0 \cdot \tilde{N}(t) \quad , \quad b(t) \neq 0 \quad . \tag{5}$$

The notion of a standard rolling for a given surface S on a *plane* turns out to be the key ingredient for the construction of approximating developable ribbons as we shall see below. To begin with, however, we first observe the following result for the more general situation of rolling S on a general surface $\tilde{S}$:

Proposition 4.2. *With the setting introduced above, suppose that the following geometric conditions are satisfied for all $t \in J$:*

$$\begin{aligned} \kappa_g(t) &= \tilde{\kappa}_g(t) \\ \kappa_n(t) &\neq \tilde{\kappa}_n(t) \quad , \end{aligned} \tag{6}$$

then g_t is a standard rolling of S on $\tilde{S}$ along γ with contact curve $\tilde{\gamma}$.

Proof. Let $R_t = \tilde{D}_t D_t^{\mathsf{T}}$ and $c_t = \tilde{\gamma}(t) - R_t\gamma(t)$. Then, $g_t(x) = R_t x + c_t$, and so we can find the instantaneous motion V_t by computing $\Omega_t(x - c_t) + c_t'$. Since $c_t' = \tilde{\gamma}'(t) - R_t'\gamma(t) - R_t\gamma'(t) = -R_t'\gamma(t)$ for R_t maps $\gamma'(t)$ to $\tilde{\gamma}'(t)$, we obtain

$$\begin{aligned} V_t(x) &= \Omega_t(x - \tilde{\gamma}(t) + R_t\gamma(t)) - R_t'\gamma(t) \\ &= \Omega_t x - \Omega_t\tilde{\gamma}(t) + R_t'\gamma(t) - R_t'\gamma(t) \\ &= \Omega_t(x - \tilde{\gamma}(t)), \end{aligned} \tag{7}$$

where $\Omega_t = R_t' R_t^{\mathsf{T}} = \tilde{D}_t'\tilde{D}_t + \tilde{D}_t D_t'^{\mathsf{T}} D_t \tilde{D}_t^{\mathsf{T}}$. If now we let

$$\Lambda_t = \|\gamma'(t)\| \begin{bmatrix} 0 & \kappa_g(t) & \kappa_n(t) \\ -\kappa_g(t) & 0 & \tau_g(t) \\ -\kappa_n(t) & -\tau_g(t) & 0 \end{bmatrix}, \tag{8}$$

we have – from equation (1) – that $\tilde{D}_t' = \tilde{D}_t\tilde{\Lambda}_t^{\mathsf{T}} = -\tilde{D}_t\tilde{\Lambda}_t$ ($\tilde{\Lambda}_t$ is skew symmetric) as well as $D_t'^{\mathsf{T}} D_t = \Lambda_t$. Hence, if $\Xi_t = \Lambda_t - \tilde{\Lambda}_t$, that is

$$\Xi_t = \begin{bmatrix} 0 & \Xi_t^{1,2} & \Xi_t^{1,3} \\ -\Xi_t^{1,2} & 0 & \Xi_t^{2,3} \\ -\Xi_t^{1,3} & -\Xi_t^{2,3} & 0 \end{bmatrix}, \tag{9}$$

where

$$\begin{aligned} \Xi_t^{1,2} &= \|\gamma'(t)\| \cdot (\kappa_g(t) - \tilde{\kappa}_g(t)) \\ \Xi_t^{1,3} &= \|\gamma'(t)\| \cdot (\kappa_n(t) - \tilde{\kappa}_n(t)) \\ \Xi_t^{2,3} &= \|\gamma'(t)\| \cdot (\tau_g(t) - \tilde{\tau}_g(t)), \end{aligned} \tag{10}$$

the expression for Ω_t reduces to

$$\Omega_t = \tilde{D}_t \Xi_t \tilde{D}_t^{\mathsf{T}}, \tag{11}$$

and the resulting angular velocity vector of the rolling is thence – with respect to the Darboux frame $\tilde{\mathcal{F}}(t) = \{\tilde{e}(t), \tilde{h}(t), \tilde{N}(t)\}$ along $\tilde{\gamma}$ in $\tilde{S}$:

$$\begin{aligned} \omega_t &= \left(-\Xi_t^{2,3},\ \Xi_t^{1,3},\ -\Xi_t^{1,2}\right)_{\tilde{\mathcal{F}}(t)} \\ &= \|\gamma'(t)\| \cdot \left(-\tau_g(t) + \tilde{\tau}_g(t),\ \kappa_n(t) - \tilde{\kappa}_n(t),\ -\kappa_g(t) + \tilde{\kappa}_g(t)\right)_{\tilde{\mathcal{F}}(t)} \quad . \end{aligned} \tag{12}$$

From (6) we then read off that the motion g_t is a standard rolling if (and only if) (5) is satisfied. □

In passing we note – for later use – that (12) and proposition 4.2 immediately give the coordinates of the pulled-back angular rotation vector $\hat{\omega}_t = R_t^{\mathsf{T}}\omega_t$ with respect to the frame $\mathcal{F}(t)$ for a standard rolling:

$$\hat{\omega}_t = \|\gamma'(t)\| \cdot (-\tau_g(t) + \tilde{\tau}_g(t)\,,\ \kappa_n(t) - \tilde{\kappa}_n(t)\,,\ 0)_{\mathcal{F}(t)} \quad . \tag{13}$$

The important special case in which $\tilde{S}$ is a plane is covered by the following corollary:

Corollary 4.3. *If $\tilde{S}$ is a plane, then the motion g_t is a standard rolling if and only if*

$$\begin{aligned} \kappa_g(t) &= \tilde{\kappa}_g(t) \\ \kappa_n(t) &\neq 0 \quad . \end{aligned} \tag{14}$$

The instantaneous angular rotation vector ω_t and its pull-back $\hat{\omega}_t$ are correspondingly – in $\tilde{\mathcal{F}}(t)$ and $\mathcal{F}(t)$ respectively:

$$\begin{aligned} \omega_t &= \|\gamma'(t)\| \cdot (-\tau_g(t), \kappa_n(t), 0)_{\tilde{\mathcal{F}}(t)} \\ \hat{\omega}_t &= \|\gamma'(t)\| \cdot (-\tau_g(t), \kappa_n(t), 0)_{\mathcal{F}(t)} \quad , \end{aligned} \tag{15}$$

where now $\tilde{\mathcal{F}}(t) = \{\tilde{e}(t), \tilde{e}_3 \times \tilde{e}(t), \tilde{e}_3\}$ is the co-moving frame in the plane with constant normal vector field $\tilde{e}_3$ along $\tilde{\gamma}$.

In the following section we show that the rolling just discussed serves as an alternative tool for obtaining a flat developable approximation of the surface S along γ:

4.1. **Developable Cartan surface ribbons.** We first consider the notion of ruled surfaces as developable surfaces constitute a special subcategory of those:

Let $w > 0$, $I = [-w, w]$, and $V = J \times I$. A *parametrized ruled surface (with boundary)* $r\colon V \to \mathbb{R}^3$ based on the center curve γ is determined by a vector field β along γ:

$$r(t,u) = \gamma(t) + u \cdot \beta(t) \quad , \ t \in J,\ u \in I. \tag{16}$$

We may assume without lack of generality (via suitable adjustment of the u-interval) that β is a unit vector field along γ. The surface r is regular when its partial derivatives are linearly independent and u is sufficiently small. Regularity implies in particular that

$$\beta(t) \neq \pm e(t) \text{ for all } t \in J. \tag{17}$$

Moreover, the surface $r(V)$ is flat (with Gaussian curvature zero at all points, i.e. developable), precisely when the following condition is satisfied – see [22, p. 194]:

$$\beta' \cdot (\beta \times e) = 0. \tag{18}$$

If $r(V)$ is eventually to be constructed so that it becomes a flat approximation of S along γ, we need to find a regular parametrization r such that $r(V)$ is developable and

has the same normal field N as S along γ. It means that we need to determine the vector function β so that it fulfills (17), (18), and

$$\beta \cdot N = 0. \tag{19}$$

It turns out that the desired vector function β is precisely (modulo length and sign) the previously encountered pulled-back angular velocity vector $\hat{\omega}_t$ along γ associated with the rolling of S along $\tilde{\gamma}$ on a plane, see [23] and [10]:

Theorem 4.4. *Let γ denote a smooth curve on a surface S and let $\mathcal{F} = \{e, h, N\}$ be the corresponding Darboux frame field along γ. Suppose that the normal curvature function κ_n for γ on S never vanishes. Then there exists a unique developable surface which contains γ and which has everywhere the same tangent plane as S along γ. It is parametrized as follows:*

$$r(t,u) = \gamma(t) + u \cdot \frac{\hat{\omega}_t}{\|\hat{\omega}_t\|} \quad , \quad u \in [w_-(t), w_+(t)] \quad , \quad t \in J. \tag{20}$$

where $\hat{\omega}_t$ denotes the pulled-back angular velocity vector:

$$\begin{aligned} \hat{\omega}_t &= \kappa_n(t) \cdot h(t) - \tau_g(t) \cdot e(t) \quad , \\ \|\hat{\omega}_t\| &= \sqrt{\kappa_n^2(t) + \tau_g^2(t)} \quad . \end{aligned} \tag{21}$$

Definition 4.5. The developable surface, which is parametrized by (20) – and which is therefore approximating the surface S – will be called the Cartan surface ribbon along γ on S.

As is already in the name, the Cartan surface ribbon can be *developed* isometrically into a planar ribbon:

Definition 4.6. The *associated Cartan planar ribbon* for γ on S – which is defined along $\tilde{\gamma}$ in the plane – is now determined via (22) in the proposition below, which also establishes the isometry between the two Cartan ribbons.

Proposition 4.7. *An isometry from the Cartan surface ribbon onto the associated Cartan planar ribbon is realized along the development curve $\tilde{\gamma}$ in the following way, which is in precise accordance with the previously found rolling of S along γ on the plane with contact curve $\tilde{\gamma}$. We simply map the point $r(t,u)$ to the point*

$$\begin{aligned} \tilde{r}(t,u) &= \tilde{\gamma}(t) + u \cdot \frac{\omega_t}{\|\omega_t\|} \\ &= \tilde{\gamma}(t) + u \cdot \frac{\omega_t}{\sqrt{\kappa_n^2(t) + \tau_g^2(t)}} \quad . \end{aligned} \tag{22}$$

Proof. We let $\beta(t) = \omega_t / \|\omega_t\|$ and $\hat{\beta}(t) = \hat{\omega}_t / \|\hat{\omega}_t\|$. Since $\kappa_g(t) = \tilde{\kappa}_g(t)$ all the scalar products between two vectors chosen from $\{\gamma'(t), \hat{\beta}(t), \hat{\beta}'(t)\}$ are the same as the scalar products between the corresponding two vectors chosen from $\{\tilde{\gamma}'(t), \beta(t), \beta'(t)\}$. It follows

that the two first fundamental forms for $r(t,v)$ and $\tilde{r}(t,v)$ respectively, have identical coordinate functions. The two ribbons r and $\tilde{r}$ are therefore isometric. □

5. Intermezzo

In view of our observations concerning the rolling of S on the plane, it now makes sense to say that the Cartan surface ribbon can be *rolled* isometrically onto the associated Cartan planar ribbon. This is induced in the way just described by the rolling of S on the plane, which itself is represented by the pulled-back angular velocity vector field $\hat{\omega}$ along γ in S and by ω along $\tilde{\gamma}$ in the plane. Accordingly, once the center curve $\tilde{\gamma}$ in the plane has been constructed using $\tilde{\kappa}_g(t) = \kappa_g(t)$, then the approximating Cartan *surface* ribbon can be obtained via the inverse rolling of the Cartan *planar* ribbon backwards into contact with the surface S along γ.

The key object for the actual construction of the approximating Cartan surface ribbon along a given curve γ on S is thence the planar curve $\tilde{\gamma}$, which may itself be constructed either by rolling, or – simpler – by integrating the curvature function κ_g of γ, but in the plane, in the well known way, see [22]:

Proposition 5.1. *Suppose $\tilde{\gamma}$ has (signed) curvature κ_g and speed $\|\tilde{\gamma}'\| = v$. Then, modulo rotation and translation in the plane, we have:*

$$\tilde{\gamma}(t) = \int_0^t v(\hat{t}) \cdot (\cos(\varphi(\hat{t}))\,,\ \sin(\varphi(\hat{t}))\, d\hat{t} \tag{23}$$

where

$$\varphi(\hat{t}) = \int_0^{\hat{t}} v(\hat{u}) \cdot \kappa_g(\hat{u})\, d\hat{u} \quad . \tag{24}$$

The curve $\tilde{\gamma}$ appears as a special – and simple – example of a *Cartan development* as already alluded to via the reference to Nomizu's initial work, see [4] and [24]. This is why the ensuing developable ribbons are called *Cartan surface ribbons*. To be a bit more specific concerning our simple 2-dimensional setting, we recall in particular the important geodesic curvature equivalence used above:

We let the tangent space $T_{\gamma(0)}S$ at $\gamma(0)$ represent the plane $\tilde{S}$ into which we want to construct the Cartan development curve corresponding to the given curve γ in S. For each t we consider the parallel transport of the tangent vector $\gamma'(t)$ along γ from the point $\gamma(t)$ to the point $\gamma(0)$, see [24] and [5, p. 131]:

$$X(t) = \Pi_{\gamma}^{\gamma(t)\,,\,\gamma(0)}\,(\gamma'(t)) \quad . \tag{25}$$

The Cartan development $\tilde{\gamma}$ of γ in $T_{\gamma(0)}S$ is then:

$$\tilde{\gamma}(t) = \int_0^t X(u)\ du \quad . \tag{26}$$

From this construction it follows in particular that

Proposition 5.2. *Any tangent vector $\tilde{\gamma}'(t_1) = X(t_1)$ is itself parallelly transported (in the usual Eucliden sense) along $\tilde{\gamma}$ in the tangent space $T_{\gamma(0)}S$ (which may be canonically identified with $T_{\tilde{\gamma}(0)}\tilde{S}$) from $(0,0)$ to $\tilde{\gamma}(t_1)$ and the (geodesic) curvature function of the planar curve $\tilde{\gamma}$ is equal to the geodesic curvature function of the original curve γ in S:*

$$\tilde{\kappa}_g(t) = \kappa_g(t) \quad \textit{for all } t. \tag{27}$$

Proof. Suppose Y is any parallel vector field along the curve γ on the surface S, then the angle $\theta(t) = \angle(Y(t), \gamma'(t))$ gives the geodesic curvature of γ via $\theta'(t) = \kappa_g(t)$. Since the same holds true by construction along the development curve $\tilde{\gamma}$ in the tangent plane, we get $\tilde{\theta}(t) = \theta(t)$ so that $\tilde{\kappa}_g = \kappa_g$. □

In the examples below – in sections 7 and 8 – the planar ribbons on display are all constructed from planar center curves $\tilde{\gamma}$ via (23) using the geodesic curvature function from the given curves γ on the respective surfaces S.

6. Gauss Bonnet inspection

We consider a finite (piecewise smooth) ribbonization $\mathcal{R} = \cup_i^R \mathcal{R}_i$, $R = \#\mathcal{R}$, of S all of whose Cartan surface ribbons $\mathcal{R}_i$, $i = 1 \cdots R$ are closed in the sense that they are based on closed smooth center curves on S as in figures 2, 4, and 7 below. Let $\mathcal{W} = \cup_i \mathcal{W}_i$ denote the system of (piecewise smooth) wedge curves stemming from the ribbonization $\mathcal{R}$ and let $\widehat{\mathcal{W}}$ denote the corresponding planar wedge curve system of the Cartan planar ribbons $\widehat{\mathcal{R}}$. The end (cut-)curves of the planar ribbons – that are typically needed in order to obtain the planar representation of the ribbons – are not considered part of $\widehat{\mathcal{W}}$.

We now apply the Gauss Bonnet theorem to surfaces which are ribbonized by such circular ribbons.

The system of wedge curves $\mathcal{W}$ consists of curves with possible branch-points, where three or more ribbons come together, and with possible end-points, where one ribbon is locally bent around the wedge (and is thus in contact with itself), as in the top and bottom ribbon on the ellipsoid in figure 6 below.

We may assume without lack of generality that the branch points and end points are all isolated and regular in the sense that the wedge curves in a neighbourhood of such points can be mapped diffeomorphically to a corresponding star configuration in $\mathbb{R}^3$ with a number of straight line segments issuing from a common vertex. The branch-points and end-points are called *vertices* of the ribbonization $\mathcal{R}$. The vertex set is denoted by $\mathcal{P}$ and the number of veritces by $P = \#\mathcal{P}$. The number of segments issuing from a given vertex p_k in the vertex set $\mathcal{P}$ is called the *degree*, $d_k = d(p_k)$ of the vertex. If a ribbon has an isolated cone point then this is also a vertex, and – in accordance with the above definition – we count its degree as 0.

Theorem 6.1. *The Euler characteristic, $\chi(\mathcal{R})$, of a ribbonization $\mathcal{R}$ is*

$$\chi(\mathcal{R}) = \frac{1}{2}\sum_{k=1}^{P}(2-d_k) \quad . \tag{28}$$

Proof. The total curvature contributions for the Gauss–Bonnet theorem can be divided into three parts:

a) *Surface contributions:* the surface integral of the Gauss curvature K,

$$C_{\mathcal{R}\setminus\mathcal{W}\cup\mathcal{P}} = \int_{\mathcal{R}\setminus\mathcal{W}\cup\mathcal{P}} K d\mu = 0 \quad . \tag{29}$$

b) *Wedge contributions:* The integral of the geodesic curvature along the edges of the Cartan ribbons excluding the vertex points. Here n_r is the number of circular Cartan ribbons,

$$C_{\mathcal{W}\setminus\mathcal{P}} = \sum_{q=1}^{R}\int_{\mathcal{W}_q\setminus\mathcal{P}_q} \kappa^{\mathcal{W}_q}(s)\, ds \quad . \tag{30}$$

c) *Vertex contributions:* sum of the angular deficit (angular defect) at the vertices, i.e. 2π minus the sum of the inner angles $\beta(j,k)$ at the vertices. The inner angles are replaced by the corresponding outer angles $\alpha(j,k)$ as $\alpha = \pi - \beta$ where $\alpha \in [-\pi, \pi]$ and $\beta \in [0, 2\pi]$,

$$\begin{aligned} C_{\mathcal{P}} &= \sum_{j=1}^{P}\left(2\pi - \sum_{k=1}^{d_k}\beta(j,k)\right) \\ &= \sum_{k=1}^{P}\left(2\pi - \sum_{j=1}^{d_k}(\pi - \alpha(j,k))\right) \\ &= \sum_{k=1}^{P}(2\pi - \pi d_k) + \sum_{k=1}^{n_v}\sum_{j=1}^{d_k}\alpha(j,k) \quad . \end{aligned} \tag{31}$$

Summarizing: Adding these contributions together we find:

$$2\pi\cdot\chi(\mathcal{R}) = \sum_{q=1}^{R}\int_{\mathcal{W}_q\setminus\mathcal{P}_q}\kappa^{\mathcal{W}_q}(s)\, ds + \sum_{k=1}^{P}\sum_{j=1}^{d_k}\alpha(j,k) + \sum_{k=1}^{P}(2\pi - \pi d_k) \quad . \tag{32}$$

By a permutation of the outer angles in the second term one can group them according to the ribbon wedge curves they appear on. This is possible because each of the kinks on the ribbons is encountered precisely once in the summation. Further, as the ribbons

are closed it follows that their wedge integral and the corresponding sum of outer angles together cancels to zero. Hence one is left with the equality:

$$\chi = \frac{1}{2}\sum_{k=1}^{P}(2 - d_k) \quad . \tag{33}$$

□

Remark 6.2. *As mentioned, the set of vertices, $\mathcal{P}$, is a feature of the three-dimensional mesh of wedge curves. Wedge curves from two, most commonly distinct, ribbons follow each other until a vertex point, where, e.g. three ribbons come together. We summarize the different vertex characters with a table (1).*

d_k	*Vertex character*	*Classification*
0	*Fully circumscribed by one ribbon*	*Cone point*
1	*Half circumscribed by a ribbon*	*Wedge end point*
2	*Two ribbons meet at the point*	*Zero contributing vertex*
> 2	$n > 2$ *ribbons meet*	*Conventional vertex.*

TABLE 1. A characterization of vertices.

Remark 6.3. *The ribbon formula in Theorem 6.1 is valid for orientable as well as non-orientable surfaces. To see this we only need to show that the formula does not change whether the ribbons are regular closed ribbons or Möbius strip-ribbons. This follows as a consequence of lemma 6.4 below. In particular, once a given non-orientable surface has been ribbonized (in the way presented above), it is straightforward both to ribbonize its corresponding double cover $\widehat{\mathcal{R}}$ and to obtain its corresponding well known modification of the Euler Characteristic, $\chi(\widehat{\mathcal{R}}) = 2 \cdot \chi(\mathcal{R})$.*

Lemma 6.4. *A conventional cylindrical closed ribbon (without vertices), and a Möbius strip-ribbon both contribute zero to the total curvature integral.*

Proof. It follows simply by cutting the ribbons along a ruler. In this case, the ribbons can be fully flattened and has a total curvature contribution of 2π which is equal to the sum of the four artificial angles introduced by the cutting along the ruler. The difference between a ribbon that is orientable and one that is not consists of a simple permutation of the four inner angles of the cut. □

6.1. **From ribbon inspection to the Euler polyhedral formula.** We consider a polyhedron Q and apply the conventional notation, i.e. F, E and V denote the number of faces, of edges, and of vertices, respectively, of the *polyhedron*. To apply the ribbon formula (28) we need to cover the polyhedron with closed ribbons. One can cover each one of the F faces by a closed ribbon with a (flat) vertex covering the intrinsic part of

the face polygon. With this choice there are then F new such virtual vertices, all with degree zero. We therefore have the total number of ribbon vertices

$$P = V + F \tag{34}$$

and

$$\sum_{k=1}^{P} d_k = 2 \cdot E \quad . \tag{35}$$

Hence we recover the well known polyhedron formula from the ribbon formula:

$$\chi(Q) = \frac{1}{2}\sum_{k=1}^{V}(2 - d_k) = \frac{1}{2}(2 \cdot (V + F) - 2 \cdot E) = V - E + F \quad . \tag{36}$$

7. Example: An unknot-based Cartan ribbonized torus

This example is concerned with the ribbonization of the torus

$$\mathcal{T}^2 \ : \ \sigma(u, v) = ((2 + \cos(u)) \cdot \cos(v)\,,\ (2 + \cos(u)) \cdot \sin(v)\,,\ \sin(u))\ ,\ (u, v) \in \mathbb{R}^2 \tag{37}$$

using the following two closed curves as center curves (see figure 1):

$$\begin{aligned} \gamma_1(t) &= \sigma\,(3 \cdot t\,,\ t) \quad , \quad t \in [-\pi, \pi] \\ \gamma_2(t) &= \sigma\left(3 \cdot t\,,\ t + \frac{\pi}{3}\right) \quad , \quad t \in [-\pi, \pi] \quad . \end{aligned} \tag{38}$$

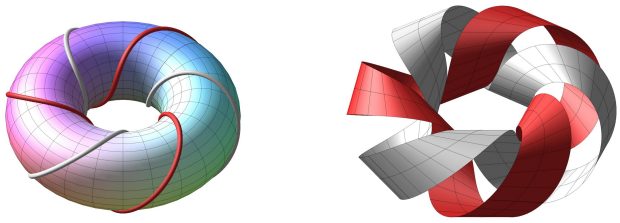

Figure 1. Two $(3, 1)$-unknots on a torus that are used as center curves for the beginning of a Cartan ribbonization of the torus. See figure 2 with the corresponding ribbons, extended and cut-off.

The corresponding two Cartan surface ribbons are then constructed (with constant and equal width functions) along the two curves, using the parametrization recipe in equation (20). They are displayed on the right in figure 1). The ribbons are then widened in $\mathbb{R}^3$ in the direction of $\pm\omega$ until intersection with their respective neighbour ribbons.

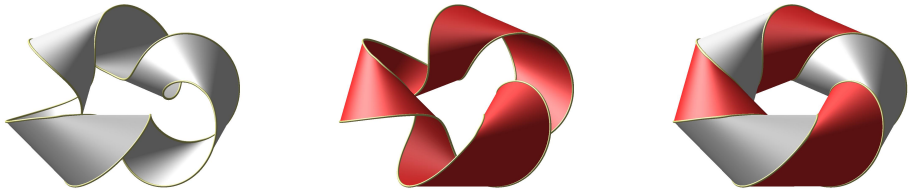

FIGURE 2. Ribbonization of the torus along two $(3,1)$-unknots with the correct cut-off width functions.

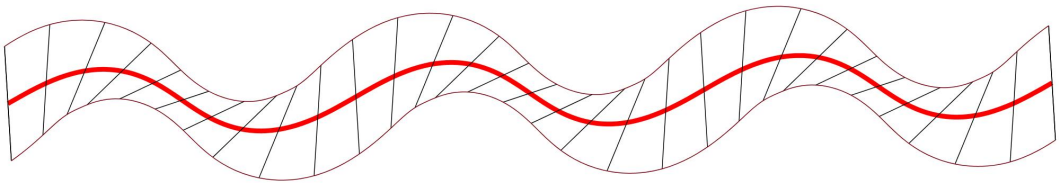

FIGURE 3. The geometry of one of the two planar ribbons used for the covering of the torus in figure 2.

The intersection width functions are obtained numerically by solving the intersection equation for each value of t along the center curves, see figure 2. Once the cut-off widths $w_\pm$ of the Cartan surface ribbons have been determined, the corresponding Cartan planar ribbons (with the same width-functions $w_\pm(t)$) are finally constructed from the planar center curve with the same geodesic curvature as the original center curve on the surface. In this particular case both Cartan planar ribbons are identical – one of them is displayed in figure 3.

8. Example: Curvature line based ribbonizations of an ellipsoid

A curvature line parametrization of the ellipsoid with half axes $\sqrt{a} > \sqrt{b} > \sqrt{c} > 0$ is obtained as follows, see [25] and in particular [9, Example 7.4]:

$$\sigma(u,v) = \left(\pm\sqrt{\frac{a(a-u)(a-v)}{(a-b)(a-c)}}\ ,\ \pm\sqrt{\frac{b(b-u)(b-v)}{(b-a)(b-c)}}\ ,\ \pm\sqrt{\frac{c(c-u)(c-v)}{(c-a)(c-b)}} \right) \quad , \tag{39}$$

where $u \in (b,a)$ and $v \in (c,b)$. This particular parametrization of the ellipsoid is shown in the leftmost display in figure 4. As shown on the display the coordinate (curvature lines) of this parametrization extend smoothly from one octant to a neighboring octant except at the 4 umbilical points on the ellipsoid corresponding to parameter values $u \to b$ and $v \to b$.

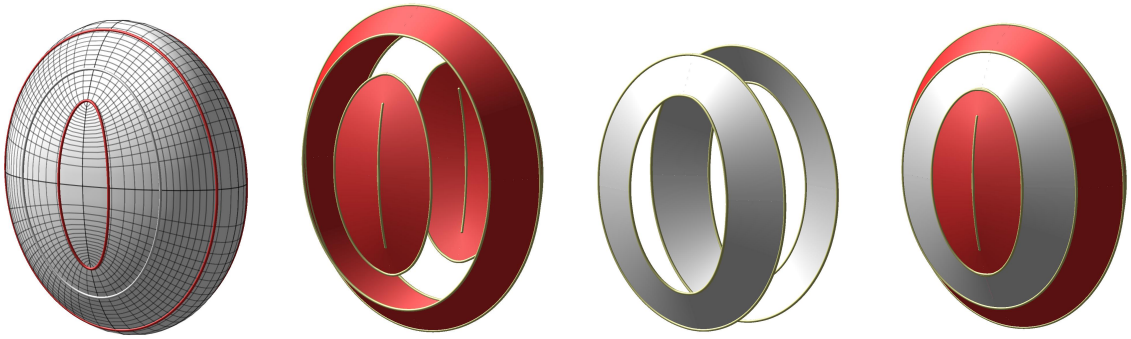

FIGURE 4. Ribbonization of the ellipsoid with half axes $\sqrt{5}$, 2, and 1 corresponding to the parameters $(a, b, c) = (5, 4, 1)$ in the representation (39). The ribbonization is built from 6 Cartan surface ribbons along the indicated line-of-curvature center-lines which intersect the horizontal "equator" at equi-distributed points.

If we restrict attention to that part of the ellipsoid which lies in the positive octant $(+, +, +)$, then every u-coordinate curve (with a fixed coordinate v) is parametrized as follows - using the positive coordinate functions in (39):

$$\gamma(t) = \sigma(t, v) \quad , \quad t \in (b, a) \quad . \tag{40}$$

Then γ has vanishing geodesic torsion $\tau_g = 0$, and the corresponding Cartan surface ribbon is therefore simply given as follows for suitable width-functions w_- and w_+:

$$r(t, u) = \gamma(t) + u \cdot h(t) \quad , \quad t \in (b, a) \ , \ u \in (w_-(t), w_+(t)) \quad . \tag{41}$$

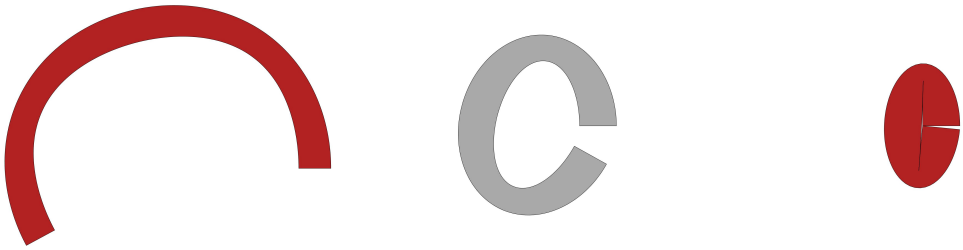

FIGURE 5. The three planar ribbons that are used for covering (half of) the ellipsoid in figure 4. In order to realize the isometry into the plane each one of them is necessarily cut by a transversal curve. In this case they are cut along the rightmost horizontal straight line which corresponds to a cutting of the surface ribbons along the equator $x = 0$, i.e. along the parameter curves $u = a$. The center curves of the planar ribbons are the development contact curves of the rollings of the ellipsoid on the plane.

The striction (singularity) curve ζ for the developable Cartan surface ribbon, which has γ as its center curve, is determined by the geodesic curvature κ_g of γ and the field h from the frame field $\mathcal{F}$ along γ as follows (for each given fixed value of the v-parameter, $v \in]c, b[$):

$$\zeta(t) = \gamma(t) + \left(\frac{1}{\kappa_g(t)}\right) \cdot h(t) \quad , \quad t \in (b, a) \quad . \tag{42}$$

A direct calculation gives:

$$\kappa_g(t) = \sqrt{\frac{(a-v)(b-v)(v-c)}{v(t-v)^3}} \quad , \tag{43}$$

and therefore:

$$\zeta(t) = \left(\sqrt{\frac{a(a-t)^3}{(a-v)(a-b)(a-c)}} \ , \ -\sqrt{\frac{b(t-b)^3}{(b-v)(a-b)(b-c)}} \ , \ \sqrt{\frac{c(t-c)^3}{(v-c)(a-b)(b-c)}} \right) ,$$

where $t \in (b, a)$ and $v \in (c, b)$. In particular, the striction curve of the Cartan surface ribbon for the center curve γ (in the octant $(+,+,+)$ is seen to be completely contained in the octant $(+,-,+)$. Therefore every pair of Cartan surface ribbons with curvature line center curves will form intersection (wedge) curves before the striction lines are met. In other words, the resulting Cartan surface ribbonization will always be regular off the wedge curves as shown in figures 4 and 7.

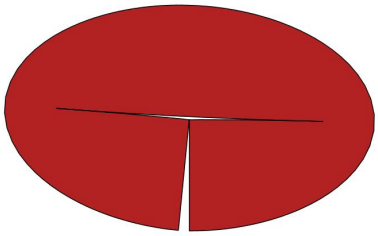

FIGURE 6. An enlargement of the right-most top cover ribbon in figure 5. When cut out from the plane the shown gaps can be simultaneously closed by an isometry into the top ribbon for the ellipsoid ribbonization. It will have two point singularities – two vertices – corresponding to the two umbilical points of the ellipsoid "below" the approximating ribbon. The ensuing curve of self-intersection in between the two point singularities is an ordinary smooth wedge segments of the ribbonization.

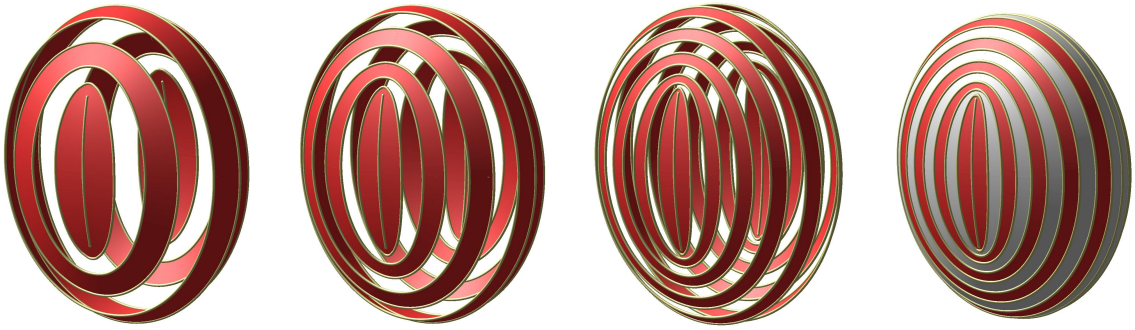

FIGURE 7. Further approximating ribbonizations of the ellipsoid in figure 4.

9. Conclusion

In this paper we recover the conditions for the existence of proper rollings of one surface on another [3-6] – in particular the condition that the two contact curves, that are generated from the rolling, have identical geodesic curvature. This follows from defining the standard rollings as rigid motions in $\mathbb{R}^3$ that are conditioned partly via their instantaneous rotation vectors and partly via the obvious condition of contact between the mentioned track curves on the respective surfaces, i.e. common speed of the contact point along the tracks and common tangent planes at the instantaneous point of contact.

Surfaces are then approximated by a mesh of ribbons. Rolling a surface on a plane and using the Cartan developments of curves allow us to construct developable ribbons that have common tangent planes everywhere along the curve of contact on the surface. In this way we may approximate the surface not just by one such developable surface but by a full set of developable ribbons. In short the surface is ribbonized by flat ribbons which have center-curve contact with the surface. This is a clear asset in comparison with the much used method of triangulations, which typically only give discrete point contact with the surface. For example, the topology of the surface can be read off from a ribbonization as easy as from a triangulation or from a Morse function foliation:

We present a particularly simple topological inspection of the ribbonized surfaces, which gives the Euler characteristic of the ribbonization – and thence also of the surface, if the ribbonization is fine enough. The ensuing topological formula for the Gauss-Bonnet theorem involves only the vertices of the ribbonization and their degrees. This is similar to the classical inspections of topology stemming from Morse theory and from the Poincaré-Hopf formula, which also amount to summing over critical point indices. If we organize the ribbonization of a given surface according to level curves of a Morse function we obtain the direct comparison shown in table 2.

The intriguing relations between the kinematics of rolling and the geometry of developable surfaces clearly carries many more assets for future work than what we cover in the present paper. As indicated above, already the study of ribbonizations could well

	Ribbon degree ($d(v_k)$)	Morse index (γ)	Vector field index (I)
Minimum	0	0	1
Saddle point	4	1	-1
Maximum	0	2	1
χ	$\frac{1}{2}\sum_{k=1}^{n_v}(2-d_k)$	$\sum_{\gamma=0}^{\gamma=2}(-1)^\gamma\, n_\gamma$	$\sum_{k=1}^{n_z} I_k$

TABLE 2. Listing the relationship between degrees of vertices, d_k, Morse indices γ, and the indices, I, of a vector field for smooth two-dimensional manifolds. Also compared are the corresponding three topological inspections for the Euler characteristic: the ribbon inspection, based on vertex counting; the Morse index formula, based on critical points of Morse functions; and the Poincaré-Hopf formula, based on the counting of types of zeros of a vector field.

pave new ways for refined analyses of physical, geometrical, and topological properties of surfaces. Not to mention the potentials of their higher dimensional analogues, and not to mention the multi-facetted applications in such diverse fields as robotics, architecture, design, and modern engineering, that they are already facilitating.

REFERENCES

[1] L. L. Schumaker.
Triangulations in CAGD.
IEEE Computer Graphics and Applications **13**, 47-52 (1993).
doi:10.1109/38.180117

[2] S. Lawrence.
Developable surfaces: Their history and application.
Nexus Network Journal **13**, 701-714 (2011).
doi:10.1007/s00004-011-0087-z

[3] D. J. Balkcom and M.T. Mason.
Robotic origami folding.
The International Journal of robotics Research **27**, 613-627 (2008).
doi:10.1177/0278364908090235

[4] K. Nomizu
Kinematics and differential geometry of submanifolds.
Tôhoku Math. Journ. **30**, 623-637 (1978).
doi:10.2748/tmj/1178229921

[5] S. Kobayashi and K. Nomizu.
Foundations of Differential Geometry I,
Interscience Publishers, New York, 1963.

[6] Y. Tunçer, M. K. Sağel, and Y. Yayli.
Homothetic motion of submanifolds on the plane in $\mathbb{E}^3$. *Journal of Dynamical Systems & Geometric theories* **5**, 57-64 (2007).
doi:10.1080/1726037X.2007.10698524

[7] L. Cui and J. S. Dai.
A Darboux-frame-based formulation of spin-rolling motion of rigid objects with point contact.

IEEE Transactions on Robotics **26**, 383-388 (2010).
doi:10.1109/TRO.2010.2040201

[8] M. G. Molina, E. Grong, and Y. Chitour.
Geometric conditions for the existence of a rolling without twisting or slipping.
Communications on Pure and Applied Analysis **13**, 435-452 (2014).
doi:10.3934/cpaa.2014.13.435

[9] S. Hananoi and S. Izumiya.
Normal developable surfaces of surfaces along curves.
Proceedings of the Royal Society of Edinburgh Section A: Mathematics pp. 1–27 (2017).
doi:10.1017/S030821051600007X

[10] M. Raffaelli, J. Bohr, and S. Markvorsen.
Sculpturing surfaces with Cartan ribbons.
In Proceedings of Bridges 2016: Mathematics, Music, Art, Architecture, Education, Culture. (pp. 457-460. Tessellations Publishing. (Bridges Conference Proceedings).
bridges2016-457

[11] L. Cui and J. S. Dai.
From sliding-rolling loci to instantaneous kinematics: An adjoint approach.
Mechanism and Machine Theory **85**, 161-171 (2015).
10.1016/j.mechmachtheory.2014.11.015

[12] Y. Chitour, M. G. Molina and P. Kokkonen.
Symmetries of the rolling model.
Mathematische Zeitschrift. **281**, 783-805 (2015).
doi:10.1007/s00209-015-1508-6

[13] Y. Tunçer and N. Ekmekci.
A study on ruled surface in euclidean 3-space.
Journal of Dynamical Systems & Geometric theories **8**, 49-57 (2010).
doi:10.1080/1726037X.2010.10698577

[14] Y. Chitour, M. G. Molina, and P. Kokkonen.
The rolling problem: overview and challenges
in Geometric Control Theory and Sub-Riemannian Geometry.
Editors: G. Stefani, J.P. Gauthier, M. Sigalotti, U. Boscain, A. Saryehev
Springer International Publishing, 2014. 103-122.
doi:10.1007/978-3-319-02132-4

[15] K. A. Krakowski and F. S. Leite.
Geometry of the rolling ellipsoid.
Kybernetika **52**, 209-223 (2016).
kybernetika2016-52-209

[16] J. Sharp.
D-forms and Developable Surfaces.
In Bridges: Mathematical Connections between Art, Music and Science (2005): 503-510.
bridges2005-121

[17] T. Wills.
D-Forms: 3D forms from two 2D sheets.
In Bridges: Mathematical Connections in Art, Music, and Science (2006) 503-510.
bridges2006-503

[18] R. R. Orduño, N. Winard, S. Bierwagen, D. Shell, N. Kalantar, A. Borhani and E..A. Akleman.
A Mathematical Approach to Obtain Isoperimetric Shapes for D-Form Construction.
In Proceedings of Bridges 2016: Mathematics, Music, Art, Architecture, Education, Culture 2016

(pp. 277-284). Tessellations Publishing.
bridges2016-277

[19] X. Ni, M. Garland and J.C. Hart.
Fair Morse functions for extracting the topological structure of a surface mesh.
ACM Transactions on Graphics (TOG) **23**, 613-622 (2004).
doi:10.1145/1186562.1015769

[20] J. W. Milnor.
Topology from the differentiable viewpoint,
The University Press of Virginia, Charlottesville (1965).

[21] A. Gray, E. Abbena, S. Salomon.
Third Edition: Modern differential geometry of curves and surfaces with Mathematica®,
ISBN: 978-0-58488-488-4. CRC Press, Boca Raton, Florida, 2006.

[22] M. P. do Carmo.
Differential geometry of curves and surfaces,
ISBN: 978-0132125895. Prentice Hall, Englewods Cliffs, New Jersey, 1976.

[23] S. Izumiya and S. Otani.
Flat Approximations of Surfaces Along Curves.
Demonstratio Mathematica **48**, 217–241 (2015).
doi:10.1515/dema-2015-0018

[24] K. Nomizu and K. Yano
On circles and spheres in Riemannian geometry.
Mathematische Annalen, **210**, 163–170 (1974).
Hyperlink

[25] J. Sotomayor and R. Garcia.
Lines of Curvature on Surfaces, Historical Comments and Recent Developments.
So Paulo Journal of Mathematical Sciences **2**, 143 (2008).
doi:10.11606/issn.2316-9028.v2i1p99-143

[1]DTU Compute, Department of Applied Mathematics and Computer Science,
[2]DTU Nanotech, Department of Micro and Nanotechnology,
Technical University of Denmark, DK-2800 Kongens Lyngby, Denmark

E-mail address: matraf@dtu.dk, jabo@nanotech.dtu.dk, stema@dtu.dk